**Title:** An Iridium(III) Complex as a Photoactivatable Tool for Oxidation of Amyloidogenic Peptides with Subsequent Modulation of Peptide Aggregation

**Authors:** Juhye Kang; Shin Jung C Lee; Jung Seung Nam; Hyuck Jin Lee; Myeong-Gyun Kang; Kyle J Korshavn; Hyun-Tak Kim; Jaeheung Cho; Ayyalusamy Ramamoorthy; Hyun-Woo Rhee; Tae-Hyuk Kwon; Mi Hee Lim



**To be cited as:** 10.1002/chem.201604751

**Link to VoR:** https://doi.org/10.1002/chem.201604751

# An Iridium(III) Complex as a Photoactivatable Tool for Oxidation of Amyloidogenic Peptides with Subsequent Modulation of Peptide Aggregation

Juhye Kang,[†[a]] Shin Jung C. Lee,[†[a]] Jung Seung Nam,[†[a]] Hyuck Jin Lee,[[b]] Myeong-Gyun Kang,[[a]] Kyle J. Korshavn,[[c]] Hyun-Tak Kim,[[a]] Jaeheung Cho,[[d]] Ayyalusamy Ramamoorthy,[[c, e]] Hyun-Woo Rhee,*[[a]] Tae-Hyuk Kwon*[[a]] and Mi Hee Lim*[[a]]

**Abstract:** Aggregates of amyloidogenic peptides are involved in the pathogenesis of several degenerative disorders. Herein, we report an iridium(III) complex, **Ir-1**, as a chemical tool for oxidizing amyloidogenic peptides upon photoactivation and subsequently modulating their aggregation pathways. **Ir-1** was rationally designed based on multiple characteristics, including (i) photoproperties leading to excitation by low-energy radiation; (ii) generation of reactive oxygen species responsible for peptide oxidation upon photoactivation under mild conditions; (iii) relatively easy incorporation of a ligand on the $Ir^{III}$ center for specific interactions with amyloidogenic peptides. Our biochemical and biophysical investigations illuminate that the oxidation of representative amyloidogenic peptides (*i.e.*, amyloid-β, α-synuclein, and human islet amyloid polypeptide) is promoted by light-activated **Ir-1**, which alters their conformations and aggregation pathways. Additionally, their potential oxidation sites are identified as methionine, histidine, or tyrosine residues. Overall, our studies of **Ir-1** demonstrate the feasibility of devising metal complexes as chemical tools suitable for elucidating the nature of amyloidogenic peptides at the molecular level as well as controlling their aggregation.

## Introduction

Amyloidogenic peptides are found in human degenerative diseases [*e.g.*, amyloid-β□(Aβ) for Alzheimer's disease, α-synuclein (α-Syn) for Parkinson's disease, human islet amyloid polypeptide (hIAPP) for type II diabetes].[1] Amyloidogenic peptides have aggregate-prone properties to form β-strand fibrils *via* oligomeric conformations, and their aggregation has been suggested to be linked to the pathogenesis of degenerative disorders.[1] Thus, a variety of approaches have been developed to regulate or suppress the aggregation pathways of amyloidogenic peptides.[1b,2] Among such methods, peptide modifications, including peptide oxidation, have been recently implicated to be a strategy suitable for modulation of amyloidogenic peptide aggregation (Figure 1a).[3]

To trigger the oxidation of peptides, some chemical reagents, such as metal ions, have been utilized.[3b,4] Metal ions are frequently used for peptide oxidation; however, they require harsh additional oxidants.[3b,4] In addition, chemical reagents capable of generating oxidants from dioxygen ($O_2$) upon photoactivation have been developed to be utilized as photosensitizers in various fields as light is a readily accessible resource.[3a,5] A series of organic molecules, such as riboflavin, rose bengal, methylene blue, and porphyrins, has been invented as photo-induced reagents;[3a,5b-h] however, (1) many of them have relatively lower quantum yields than photoactivatable transition metal complexes;[6] (2) some organic agents are rather less stable, potentially indicating their degradation upon irradiation.[5a,5i] Photoactivatable metal complexes present relatively high quantum yields, structural stability, and tunable geometries and properties upon ligand substitution.[5a,5i] Due to these beneficial aspects, multiple metal complexes have been designed and mediated for photo-induced oxidation of peptides.[5j-m] One of the inorganic complexes, $[Ru(bpy)_3]^{2+}$, has been frequently employed for oxidative modifications of peptides with light exposure.[5k-m] To achieve peptide oxidation, however, this Ru(II) complex still needs an additional electron acceptor (*e.g.*, ammonium persulfate) which could lead to cytotoxicity limiting its applications.[5k-m,7] Thus, robust inorganic complexes able to efficiently oxidize peptides simply by light introduction without the assistance of harsh additives, would be of significant value for gaining a greater understanding of peptide-related chemistry and biology.

Herein, we report an $Ir^{III}$ complex, **Ir-1** (Figure 1b), as a chemical tool for oxidation of amyloidogenic peptides with subsequent control of their aggregation under mild conditions that only include readily available $O_2$ and visible light. **Ir-1** was rationally designed as such a tool through incorporating the general properties of $Ir^{III}$ complexes previously reported for various applications, including photoactivation, formation of

[a] Juhye Kang, Dr. Shin Jung C. Lee, Jung Seung Nam, Myeong-Gyun Kang, Hyun-Tak Kim, Prof. Dr. Hyun-Woo Rhee, Prof. Dr. Tae-Hyuk Kwon and Prof. Dr. Mi Hee Lim
Department of Chemistry
Ulsan National Institute of Science and Technology (UNIST)
Ulsan 44919 (Republic of Korea)
E-mail: mhlim@unist.ac.kr (M. H. Lim), kwon90@unist.ac.kr (T.-H. Kwon), and rhee@unist.ac.kr (H.-W. Rhee).
[b] Dr. Hyuck Jin Lee
School of Life Sciences, UNIST
[c] Kyle J. Korshavn, Prof. Dr. Ayyalusamy Ramamoorthy
Department of Chemistry, University of Michigan
Ann Arbor, MI 48109 (USA)
[d] Prof. Dr. Jaeheung Cho
Department of Emerging Materials Science
Daegu Gyeongbuk Insititute of Science and Technology (DGIST)
Daegu 42988 (Republic of Korea)
[e] Prof. Dr. Ayyalusamy Ramamoorthy
Biophysics, University of Michigan
Ann Arbor, MI 48109 (USA)

† These authors contributed equally to this work.

Supporting information for this article is given *via* a link at the end of the document.

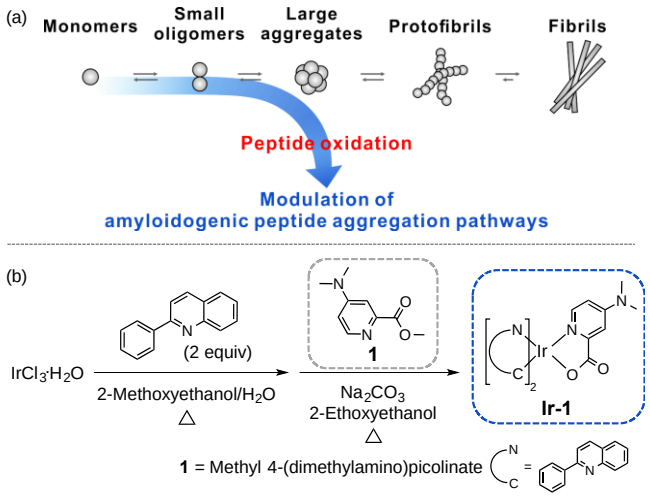


**Figure 1.** Schematic description of amyloidogenic peptide aggregation and chemical structures of **Ir-1** and **1**. As shown in (a), oxidation of amyloidogenic peptides could control their aggregation pathways. (b) Synthetic routes to **Ir-1**.

reactive oxygen species (ROS) upon light exposure, and relatively stable octahedral geometry, as well as relatively easy introduction of a ligand containing a structural moiety, suggested to be important for interactions with amyloidogenic peptides, on the $Ir^{III}$ center.[5a,8] The representative amyloidogenic peptides (*i.e.*, Aβ, α-Syn, and hIAPP) were indicated to be noticeably oxidized upon treatment of **Ir-1** with photoactivation under aerobic conditions, monitored by electrospray ionization mass spectrometry (ESI-MS), and their oxidation sites (as potential sites, methionine, histidine, and tyrosine residues) were identified by tandem MS ($ESI\text{-}MS^2$). Even with oxidative modifications of a few residues in these amyloidogenic peptides, their aggregation pathways were noticeably modulated presenting the distinct morphological features (*e.g.*, smaller-sized or amorphous peptide species, instead of fibrils (Figure 1a)). Taken together, our rational design and investigations of **Ir-1** illustrate the potential of transition metal complexes to be invented as chemical tools for oxidative modifications of amyloidogenic peptides simply employing light and $O_2$. In addition, our studies corroborate that small changes in amyloidogenic peptides, such as oxidation at a few specific residues, are able to transform overall peptide aggregation pathways, which suggests novel and viable directions for amyloid management (Figure 1a).

## Results and Discussion

### Rational design of Ir-1 for oxidation of amyloidogenic peptides

For oxidation of amyloidogenic peptides simply upon photoactivation under mild conditions, **Ir-1** (Figure 1b) was rationally designed as a chemical tool taking into account of the characteristics found in previously reported photoactivatable $Ir^{III}$ complexes as well as the specificity for amyloidogenic peptides: (i) photoproperties with relatively low-energy radiation (*i.e.*, visible light);[8d,8e] (ii) the ability to produce ROS [*e.g.*, singlet oxygen ($^1O_2$)] from redundant $O_2$, responsible for peptide oxidation, upon photoactivation;[5a,8c] (iii) a robust octahedral coordination which can provide relative structural stability without any structural modifications when light is introduced;[8c] (iv) the strong spin-orbit coupling of the $Ir^{III}$ center which could facilitate electronic transitions without the assistance of additional electron accceptors;[8d,8e] (v) incorporation of the ligand (**1**) containing a dimethylamino group, suggested to be crucial for interactions with amyloidogenic peptides,[8a,8b] onto the $Ir^{III}$ center (Figure 1b).

**Ir-1** was obtained with a relatively high yield (*ca.* 80%) through previously known two-step procedures with slight modifications as depicted in Figure 1b.[9] Moreover, **Ir-1** is easily photoactivatable under mild conditions [*e.g.*, excitation using visible light ($\varepsilon$(463 nm) = 5.78 (± 0.12) x $10^3$ $M^{-1}cm^{-1}$; Table S1 in Supporting Information) and aerobic conditions] showing its quantum yield for phosphorescence [$\Phi_p$ = 0.41 (± 0.02); Table S1 in Supporting Information]. The ability of **Ir-1** to generate singlet oxygen ($^1O_2$) from triplet dioxygen ($^3O_2$) was also confirmed by determining the quantum yield of $^1O_2$ [$\Phi_s$ = 0.25 (± 0.03); Table S1 in Supporting Information]. Overall, an octahedral $Ir^{III}$ complex, **Ir-1**, was constructed as a photoactivatable tool to oxidize amyloidogenic peptides without need of harsh conditions, prepared *via* relatively easy synthetic routes with a high yield, and demonstrated to generate oxidants (*i.e.*, $^1O_2$) from readily accessible $O_2$.

### Oxidative modifications of amyloidogenic peptides by Ir-1

In order to investigate whether the oxidation of amyloidogenic peptides by **Ir-1** under aerobic conditions would occur with light activation, three amyloidogenic peptides (*i.e.*, Aβ, α-Syn, and hIAPP found in Alzheimer's disease, Parkinson's disease, and type II diabetes, respectively) were chosen as the representative amyloidogenic peptides, and the resultant monomeric peptide species upon treatment with **Ir-1** were first monitored using ESI-MS (Figure 2). These three amyloidogenic peptides were observed to be oxidized with the addition of light-activated **Ir-1** under aerobic conditions. Without light even in the presence of **Ir-1**, all amyloidogenic peptides were in nonoxidized forms (Figure 2, middle, gray). In the case of $Aβ_{40}$, the oxidized Aβ monomers had a 16 Da increase in mass from nonoxidized peptides, implying the incorporation of one oxygen atom into the peptide (Figure 2a, bottom, blue). Note that the ligand **1** alone was not able to oxidize $Aβ_{40}$ (Supporting Information, Figure S1). Similar to $Aβ_{40}$, the doubly oxidized α-Syn with a 32 Da increase in mass, compared to the native peptide, was indicated, suggesting introduction of two oxygen atoms into the peptide (Figure 2b, bottom, blue). Slightly different from both Aβ and α-Syn, the singly oxidized monomeric hIAPP presented a 14 Da difference in mass from nonoxidized peptides (Figure 2c, bottom, blue). A 14 Da increase in mass could be resulted from the addition of one oxygen atom into hIAPP, along with the deprotonation.[3a,5f,10]

Second, we examined whether amyloidogenic peptide oligomers (focusing on Aβ oligomers) by **Ir-1** could be oxidized

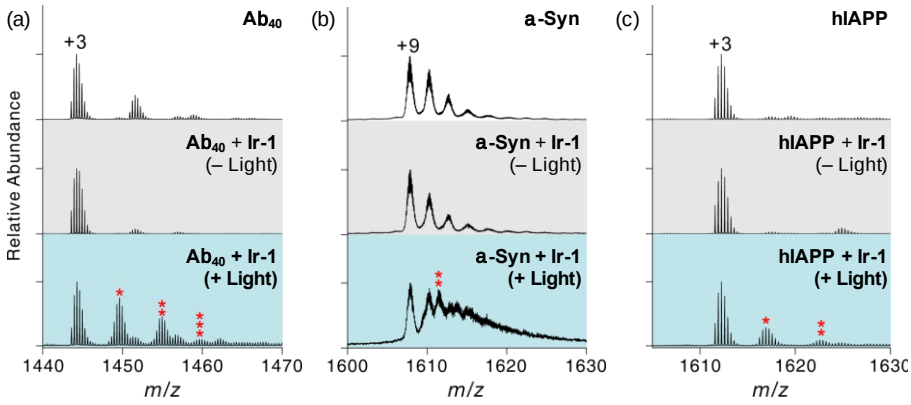


**Figure 2.** Oxidation of amyloidogenic peptides by **Ir-1** upon light activation. Mass spectrometric analyses of amyloidogenic peptides [(a) $A\beta_{40}$, (b) α-Syn, and (c) hIAPP] upon treatment with **Ir-1** in the presence of light. Oxidized peptide ions are indicated with red asterisks, and the number of asterisks indicates the number of oxygen atoms incorporated into the peptides. Conditions: [peptide] = 100 μM; [**Ir-1**] = 500 μM; pH 7.4; 37 °C; 1 h; no agitation; 1 sun light for 10 min (for the samples treated with light); aerobic conditions. Details for the assignment of oxidized peaks are included in Experimental Section.

with light activation under aerobic conditions. From the samples containing Aβ and **Ir-1** upon exposure of light and $O_2$, the oxidation of both dimers and larger oligomers was exhibited (Figure 3a and Supporting Information, S2). As demonstrated in Figure 3a, multiple oxygen atoms (*e.g.*, for dimers, up to seven oxygen atoms) were indicated to be incorporated into the oxidized oligomers.

Moreover, structural changes of monomeric and oligomeric peptide species accompanied by oxidation were probed using ion mobility mass spectrometry (IM-MS) which enables to characterize conformations based on the mobility of ions passing through a cell filled with neutral gas.[11] In the case of Aβ monomers, there was no remarkable difference in arrival time distributions (ATDs) between singly oxidized and nonoxidized $A\beta_{40}$ monomers (Supporting Information, Figure S3). Distinguishable from Aβ monomers, a change in the IM-MS data of $A\beta_{40}$ dimers upon oxidation was presented at two dominant ATDs, centered at 10.80 and 15.55 ms, respectively (Figure 3b). Nonoxidized $A\beta_{40}$ dimers exhibited the higher dominance in the larger ATD while the oxidized dimers had the opposite tendency, which suggested that peptide oxidation could lead to structural compaction in the dimers. Although the structural details of oxidized dimers had not been elucidated, their structural compaction might assist in modulating peptide aggregation as previous studies indicated that conformationally compact Aβ species could alter peptide aggregation pathways forming amorphous aggregates.[2b-2e]

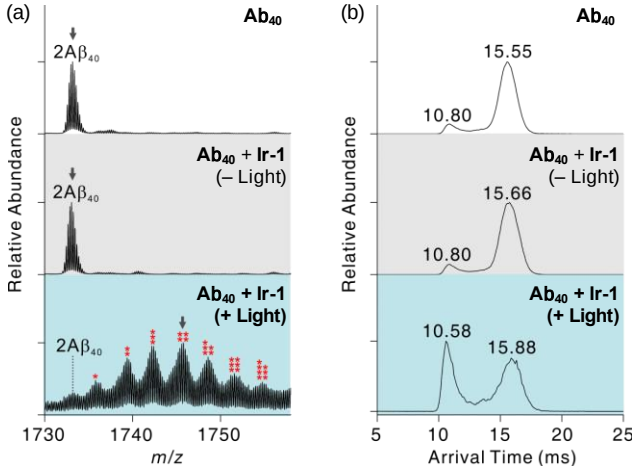


**Figure 3.** Oxidation of $A\beta_{40}$ dimers by **Ir-1** upon photoactivation. (a) ESI-MS spectra for +5-charged dimers with **Ir-1** in the absence and presence of light. The oxidized dimers are only detected by **Ir-1** with light exposure (bottom, blue). The number of red asterisks indicates the number of the oxygen atoms incorporated into $A\beta_{40}$ dimers. (b) ATDs for nonoxidized (top and middle) and tetraoxidized dimers (bottom). Each ion selected for IM-MS analysis is pointed with gray arrows in (a). The oxidized dimer incorporated with four oxygen atoms presents higher abundance in the distribution with short drift time (bottom) than nonoxidized $A\beta_{40}$ (top and middle), implying that structural compaction can be induced by oxidation. Conditions: [$A\beta_{40}$] = 100 μM; [**Ir-1**] = 500 μM; pH 7.4; 37 °C; 1 h; no agitation; 1 sun light for 10 min (for the samples treated with light); aerobic conditions.

Furthermore, the oxidation of a nonamyloidogenic structured protein, ubiquitin, was also investigated when **Ir-1** was added with light under aerobic conditions. Ubiquitin was selected as an archetypal structured protein because all secondary structures (*e.g.*, α-helix, β-strand, and random coil) could be found in ubiquitin.[12] Ubiquitin treated with **Ir-1** was shown to be oxidized with light exposure under aerobic conditions (Supporting Information, Figure S4, bottom, blue); however, the oxidized ubiquitin was significantly less abundant compared to the oxidized forms of intrinsically disordered amyloidogenic peptides (*i.e.*, $A\beta_{40}$, α-Syn, and hIAPP). Overall, oxidative modifications of amyloidogenic peptides, lacking ordered structures, are more readily achieved over structured peptides by **Ir-1** under mild conditions, including light and $O_2$, which could direct structural compaction, supporting the utilization of **Ir-1** as a photoactivatable tool for oxidation of amyloidogenic peptides.

**Identification of oxidation sites in amyloidogenic peptides**

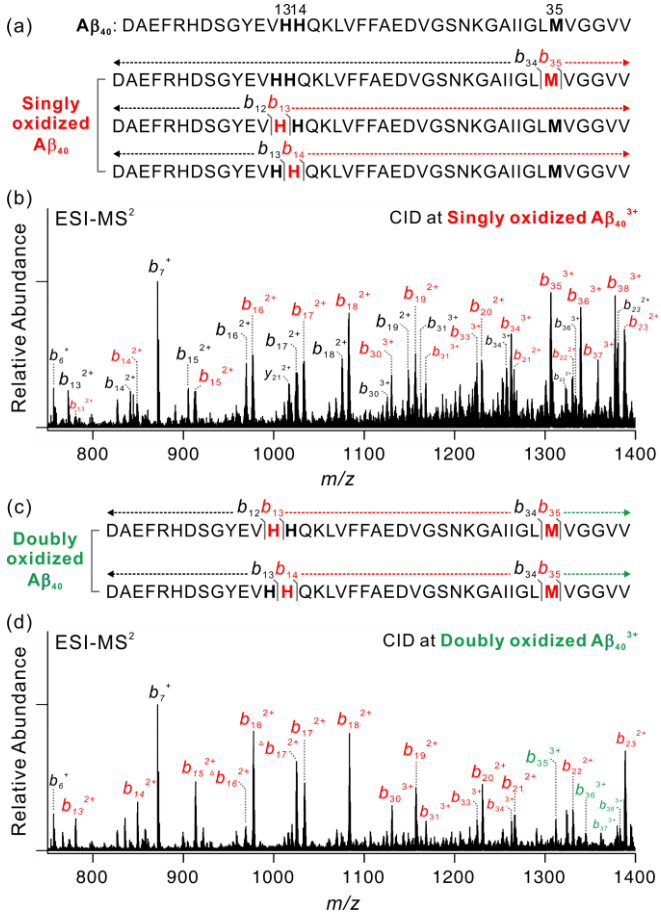


**Figure 4.** Identification of the oxidation sites in Aβ$_{40}$. (a and c) The peptide sequence and annotation for ESI-MS$^2$ and (b and d) ESI-MS$^2$ spectra for singly and doubly oxidized Aβ$_{40}$. Singly and doubly oxidized *b* fragments (N-terminal fragment ions) or *y* fragments (C-terminal fragment ions) are notated in red and green, respectively. The peaks assigned with triangles ($b_{16}$ and $b_{17}$) indicate that the loss of a water molecule occurs at serine, threonine, glutamate, or aspartate residues in these fragment ions.[13]

The resultant oxidized amyloidogenic peptides, generated by addition of **Ir-1** with light exposure under aerobic conditions, were further studied by ESI-MS$^2$, a general technique to verify the location of peptide modifications, to determine the oxidation sites in the peptides.[2d,2e] The fragment ions generated by selectively applying the collisional energy to the singly and doubly oxidized amyloidogenic peptides were analyzed. First, mapping the oxidation sites in Aβ$_{40}$ was carried out. The singly oxidized fragments, highlighted in red, were observed in *b* fragments which were cleaved from the N-terminus (Figure 4b). All *b* fragments smaller than $b_{13}$ existed as nonoxidized forms while those larger than $b_{34}$ represented only oxidized fragments. Methionine 35 (M35) is known to be the most readily oxidizable amino acid in Aβ.[3j] If the oxidation occurred only at M35, all fragments smaller than $b_{35}$ should not be oxidized (Figure 4a); however, the oxidized *b* fragments were indicated in smaller than $b_{35}$, implicating the existence of other oxidation sites (Figure 4b). Based on previous reported studies, other possible oxidation sites could be histidine residues (*i.e.*, H13, H14).[4d,14]

In the ESI-MS$^2$ spectrum for the doubly oxidized Aβ$_{40}$, there was no oxidized fragment smaller than $b_{13}$ (Figure 4d). As fragments from $b_{13}$ to $b_{34}$ only existed in singly oxidized forms (highlighted in red), this region would include one oxidation site, possibly H13 or H14. All fragments larger than $b_{34}$ were doubly oxidized (noted in green), which implied the incorporation of one oxygen atom into M35 generating a sulfoxide form (Figure 4c and 4d).

For further analysis of the oxidation sites in Aβ, the **Ir-1**-treated Aβ$_{40}$ in the absence and presence of light was evaluated by 2D band-selective optimized flip-angle short transient heteronuclear multiple quantum correlation (SOFAST-HMQC) NMR spectroscopy (Figure 5 and Supporting Information, S5). In the absence of light, minimal chemical shift perturbations (CSPs) of uniformly $^{15}$N-labeled Aβ$_{40}$ appeared upon incubation with **Ir-1** (Figure 5b), implicating no significant interaction of **Ir-1** with the peptide. Following exposure of the Aβ samples containing **Ir-1** to light, a dramatic increase of the CSPs at V12, D23, and M35 was exhibited (Figure 5c). A noticeable change in the CSP of M35 suggests that there are interactions near M35, which is consistent with the observation monitored by ESI-MS$^2$. In the case of histidine residues, though they were not well resolved within the spectra due to peak overlap, the enhanced CSP of V12, proximately located to H13 or H14, could be expected, which proposed oxidative modifications at H13 or H14, as shown in our ESI-MS$^2$ studies. Note that in the NMR spectra, D23 was adjacent to M35 with some overlaps so the shift of M35 might affect its CSP. Together, our NMR data support that Aβ$_{40}$ is oxidized at specific sites (potentially, M35, H13, H14) by **Ir-1** upon light stimulation under aerobic conditions.

Potential oxidation sites in the other amyloidogenic peptides

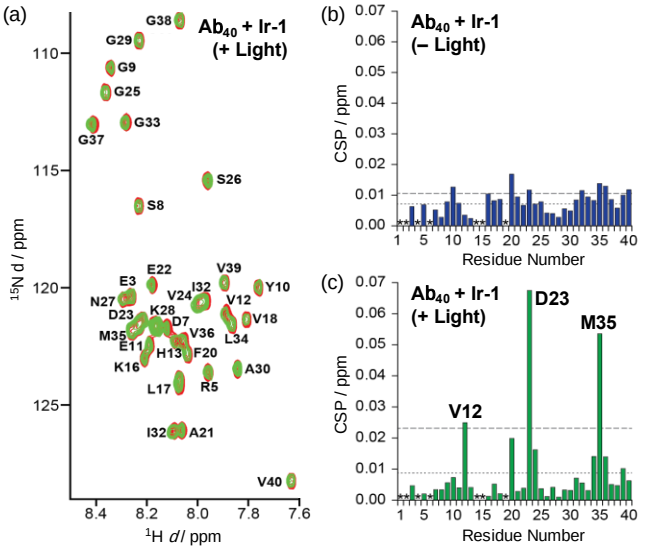


**Figure 5.** SOFAST-HMQC NMR studies of uniformly-$^{15}$N-labeled Aβ$_{40}$ monomer upon treatment with **Ir-1** with and without light. (b and c) The chemical shift perturbations (CSPs) for each spectrum (in the absence (Supporting Information, Figure S5) or presence of light (a)), relative to the spectrum of Aβ$_{40}$ without **Ir-1**, were calculated. Conditions: [$^{15}$N-labeled Aβ$_{40}$] = 80 μM; [**Ir-1**] = 160 μM; pH 7.4; 37 °C; ambient light for 1 h (for the samples treated with light); aerobic conditions. *Residues could not be resolved for analysis.

(*i.e.*, α-Syn and hIAPP), when being treated with **Ir-1** in the presence of light under aerobic conditions, were also investigated using ESI-MS$^2$ (Figure 6). When the collisional energy was applied at the doubly oxidized α-Syn (Figure 6a and 6b), no oxidation was found in small N-terminal fragments, reflecting that the oxidation at M1 and M5 rarely occurred. The C-terminal fragment $y_{13}$ was detected in a nonoxidized form, but $b_{119}$ was present in both oxidized and nonoxidized forms. One oxidation site existed between P120 and M127, and the most plausible location was M127. As singly oxidized $b_{116}$ and $b_{119}$ ions were relatively abundant, M116 was also estimated to be possibly oxidized. There were oxidized fragments smaller than $b_{116}$, such as $b_{63}$, $b_{65}$, and $b_{66}$, which implicated that there were other oxidation sites other than M116 and M127. Based on our

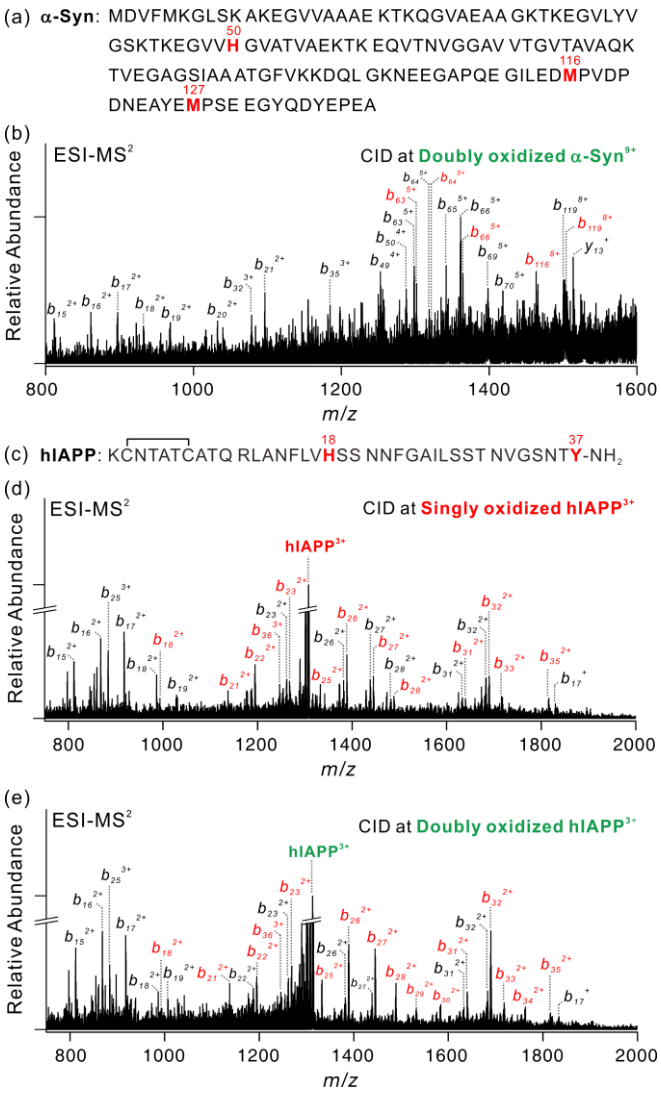


**Figure 6.** Identification of oxidation sites in α-Syn and hIAPP. Sequences of (a) α-Syn and (c) hIAPP. ESI-MS$^2$ spectra for (b) doubly oxidized α-Syn as well as (d) singly and (e) doubly oxidized hIAPP. Nonoxidized, singly oxidized, and doubly oxidized fragments are indicated in black, red, and green, respectively.

investigations for oxidation sites in Aβ$_{40}$, the histidine residue in α-Syn (*i.e.*, H50) could be an oxidation. Additionally, in the ESI-MS$^2$ spectra of singly and doubly oxidized hIAPP (Figure 6c-e), peptide oxidation was observed in fragments larger than $b_{18}$, indicative of H18 as a potential oxidation site. The fragments between $b_{18}$ and $b_{32}$, however, appeared in both oxidized and nonoxidized forms, suggesting that there was another oxidation site other than H18. Through the spectrum of doubly oxidized hIAPP (Figure 6e), no doubly oxidized ion was displayed other than the whole peptide itself, which possibly revealed that Y37 might be the second oxidation site.

Previous studies proposed that methionine, histidine, and tyrosine residues in amyloidogenic peptides are susceptible to oxidative modifications, which could affect their aggregation behaviors.[3e,3h,3j,15,16] Particularly, oxidative modifications of methionine residues have been reported to inhibit the β-strand formation of amyloidogenic peptides.[3h,3j,15] Incorporation of the oxygen atoms into methionine residues could provide their partial negative charges and further enhance the polarity of peptides.[3c,3h,15] In the case of Aβ, the increased polarity of oxidized M35 could reduce hydrophobic contacts in the C-terminal region and destabilize a β-strand structure where M35 proximately interacts with the aromatic ring of F19.[3h,15] Along with a change in polarity, the greater structural disorderness and reduced helicity were also found in methionine-oxidized α-Syn.[3c,17] Specifically, the oxidation at M116 and M127 presumably disrupts α-Syn aggregation since they are suggested to mediate long-range interactions with the hydrophobic central regions.[18] Another important oxidation sites are histidine residues. Due to its structural features, such as an imidazole ring and two protonation states, histidine has versatile roles in multiple interactions (*e.g.*, cationic–π interactions, π–π stacking, hydrogen–π interactions, coordination, and hydrogen bonding).[19] Depending on pH, histidine can present different protonation states which have effects on the molecular behaviors of amyloidogenic peptides, including their aggregation, *via* alteration of the strength of interactions.[19,20] In addition, histidine is known as metal binding sites in amyloidogenic peptides.[21] Binding of metal ions [*e.g.*, Cu(II), Zn(II)] to peptides is shown to accelerate amyloidogenic peptide aggregation or induce the formation and stabilization of toxic oligomeric aggregates.[1b,21b,21c,22] Upon formation of 2-oxo-histidine, metal binding affinities were reported to be substantially decreased; thus, oxidative modifications of histidine residues might destabilize complexes of amyloidogenic peptides with metal ions.[21e,23] Collectively, the potential oxidation sites of Aβ, α-Syn, or hIAPP as methionine, histidine, and tyrosine residues, suggested to be essential for properties and aggregation of these amyloidogenic peptides, were indicated by our MS and NMR studies. Oxidative modifications are present at a few specific residues in amyloidogenic peptides, which could be enough to modulate their aggregation pathways potentially through altering intramolecular or intermolecular interactions critical for β-strand formation (*vide infra*).

**Aggregation behaviors influenced upon oxidation of amyloidogenic peptides by light-activated Ir-1**

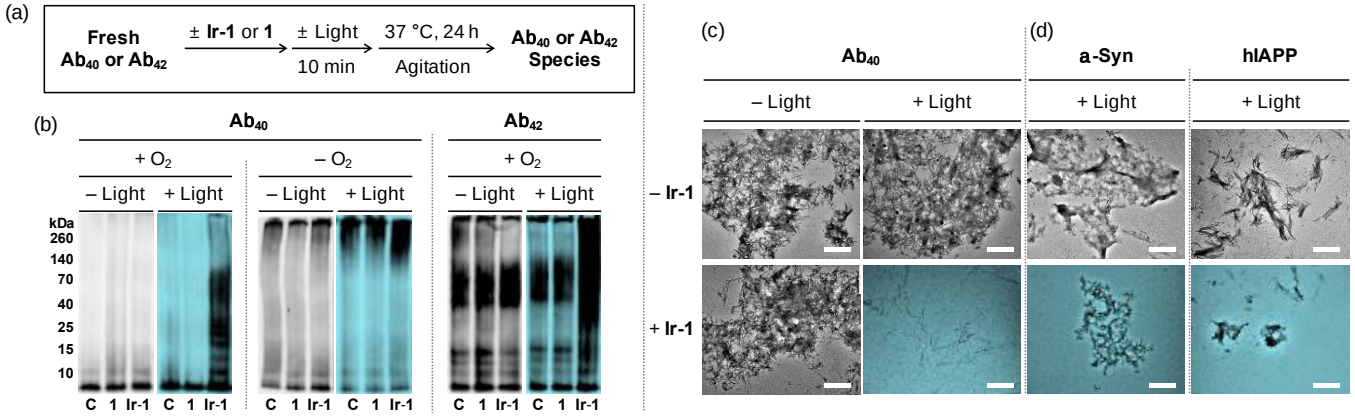


**Figure 7.** Effects of **Ir-1** and **1** on peptide aggregation pathways. (a) Scheme of the inhibition experiments. (b) Analyses of the resultant $A\beta_{40}$ and $A\beta_{42}$ species generated from various conditions [aerobic (left) and anaerobic (right) conditions] by gel/Western blot with an anti-Aβ antibody (6E10). Lanes: (C) $A\beta_{40}$ or $A\beta_{42}$; (1) $A\beta_{40}$ or $A\beta_{42}$ + **1**; (Ir-1) $A\beta_{40}$ or $A\beta_{42}$ + **Ir-1**. (c and d) TEM images of (c) the samples from (b) and (d) the light-treated samples containing α-Syn or hIAPP with and without **Ir-1** (scale bar = 1 μm). Conditions: [peptide] = 25 μM; [**Ir-1** or **1**] = 50 μM; pH 7.4; 37 °C; 24 h; constant agitation; 1 sun light for 10 min (for the samples treated with light).

**(i) Changes in size distribution.** In order to investigate whether peptide oxidation could transmute the aggregation of amyloidogenic peptides, two inhibition (Figure 7a and Supporting Information, Figure S6a) and disaggregation (Supporting Information, Figure S7a) experiments were carried out mainly using Aβ (two isoforms, $A\beta_{40}$ and $A\beta_{42}$).[2b-2e] Size distributions of the resultant $A\beta_{40}$ and $A\beta_{42}$ species treated with **Ir-1** were evaluated by gel electrophoresis with Western blotting (gel/Western blot) using an anti-Aβ antibody (6E10).

In the inhibition studies (Figure 7a), when fresh $A\beta_{40}$ was incubated with **Ir-1** in the presence of light under aerobic conditions, various molecular weights (MWs) of peptide species were visualized in the gel/Western blot (Figure 7b, left). Distinct from the result with light exposure, **Ir-1** could not generate diverse sizes of Aβ aggregates without light. In addition, when the ligands, **1** and 2-phenylquinoline (Figure 1b), were not coordinated to the $Ir^{III}$ center, they had no noticeable effect on Aβ aggregation even with light under aerobic conditions (Figure 7b and Supporting Information, Figure S6). When **Ir-1** was incubated with fresh $A\beta_{42}$, similar reactivity trends were presented to those with $A\beta_{40}$ (Figure 7b, right). Diverse MW distributions of $A\beta_{42}$ species were shown with both **Ir-1** and light. Furthermore, the inhibition experiments were conducted in the absence of $O_2$ to verify if Aβ aggregation could be influenced upon oxidation of peptides by oxidants generated by $O_2$ with light-activated **Ir-1**. Aβ aggregation pathways were not indicated to be varied under anaerobic conditions even in the presence of light (Figure 7b, middle).

Moreover, in order to disassemble preformed $A\beta_{40}$ aggregates or redirect their further aggregation upon oxidation using **Ir-1** with being light and $O_2$ present, the disaggregation experiment was carried out (Supporting Information, Figure S7). Similar to the inhibition studies, preformed $A\beta_{40}$ aggregates were observed in a wide range of sizes only after treatment with **Ir-1** upon light exposure in the presence of $O_2$. Overall, our gel/Western blot results from both inhibition and disaggregation experiments suggest that (i) **Ir-1** is able to transmute Aβ aggregation pathways only with light activation under aerobic conditions; (ii) the overall structure of **Ir-1** over individual structural components (*e.g.*, ligand **1**) is essential to alter Aβ aggregation in the presence of both light and $O_2$. Combining the results with the control of light and $O_2$, it is demonstrated that Aβ oxidation, triggered by photoactivated **Ir-1** with $O_2$, could direct modulation of peptide aggregation pathways.

**(ii) Morphological changes of amyloidogenic peptides.** The degree of regulating amyloidogenic peptides' aggregation pathways was also monitored through morphological changes which were visualized by transmission electron microscopy (TEM) (Figure 7c and 7d). From the analyses by TEM, the resultant peptides upon treatment with both **Ir-1** and light under aerobic conditions were observed to be smaller, while either structured fibrils or large aggregates were indicated without light. In the case of $A\beta_{40}$, the treatment of **Ir-1** to the peptide induced the formation of short and thin fibrils in the presence of both light and $O_2$ (Figure 7c). Additionally, the morphologies of α-Syn and hIAPP were also transformed to smaller amorphous aggregates when **Ir-1** was added with exposure of both light and $O_2$, instead of large aggregates or fibrils produced in the absence of **Ir-1** (Figure 7d). Therefore, along with the gel/Western blot data, our TEM studies imply that the aggregation of amyloidogenic peptides could be transfigured upon treatment with light-activated **Ir-1** under aerobic conditions.

## Conclusions

Several strategies for understanding and suppressing the aggregation of amyloidogenic peptides, found in amyloid-related disorders and suggested to be linked to their pathogenesis, have been developed. One of the tactics would be related to oxidative modifications of the amino acid residues essential for properties and aggregation behaviors of peptides. For peptide oxidation toward amyloidogenic peptides, an inorganic complex, **Ir-1**, rationally designed to be a chemical tool which has a relatively

stable framework and is capable of generating oxidants (*e.g.*, $^1O_2$) from readily accessible $O_2$ simply upon photoactivation using low-energy radiation.

On the basis of our biochemical and biophysical analyses, **Ir-1** is shown to significantly induce oxidative modifications of amyloidogenic peptides, such as Aβ, α-Syn, and hIAPP, followed by alteration of their aggregation pathways. Peptide oxidation by photoactivated **Ir-1** is more noticeable for amyloidogenic peptides over well-structured nonamyloidogenic peptides. Employing MS and NMR, the oxidation sites are indicated to be potentially located at methionine, histidine, or tyrosine residues in these amyloidogenic peptides. Through minor alterations at a few specific residues in peptides using photoactivated **Ir-1** under mild conditions, their aggregation pathways are able to be modulated. Overall, our rational design and fundamental investigations of **Ir-1** demonstrate the promise of an inorganic complex in being developed as a chemical tool for oxidative modifications of amyloidogenic peptides and subsequent modulation of their aggregation. Such a tool will assist in advancing our fundamental understanding toward amyloidogenic peptides as well as providing insight into development of effective approaches for amyloid management.

## Experimental Section

### Materials and Methods

All reagents were purchased from commercial suppliers and used as received unless otherwise noted. Compound **1** (**1** = methyl 4-(dimethylamino)picolinate)[24] and the cyclometalated chloride-bridged $Ir^{III}$ dimers ($[Ir(C^\wedge N)_2(\mu\text{-}Cl)]_2$)[25] were prepared following previously reported procedures. Analyses of synthesized organic and inorganic materials by NMR, FT-IR, HRMS, and elemental analyzer were conducted on an Agilent 400-MR DD2 NMR spectrometer, Varian Cary 620/670 FT-IR spectrometer (UNIST Central Research Facilities, Ulsan, Republic of Korea), a JEOL JMS-700 high resolution mass spectrometer (HRMS; The Cooperative Laboratory Center of Pukyong National University, Busan, Republic of Korea), and Leco Truspec Micro (UNIST Central Research Facilities, Ulsan, Republic of Korea), respectively. $Aβ_{40}$ and $Aβ_{42}$ were purchased from Anygen ($Aβ_{40}$ = DAEFRHDSGYEVHHQKLVFFAEDVGSNKGAIIGLMVGGVV; Nam-myun, Jangseong-gun, Republic of Korea) and AnaSpec ($Aβ_{42}$ = DAEFRHDSGYEVHHQKLVFFAEDVGSNKGAIIGLMVGGVVIA; Fremont, CA, USA), respectively. α-Syn was purchased from Anaspec (α-Syn = MDVFMKGLSKAKEGVVAAAEKTKQGVAEAAGKTKEGVLYVGSKTKEGVVHGVATVAEKTKEQVTNVGGAVVTGVTAVAQKTVEGAGSIAAATGFVKKDQLGKNEEGAPQEGILEDMPVDPDNEAYEMPSEEGYQDYEPEA; Fremont, CA, USA). hIAPP was obtained from Peptron (hIAPP = KCNTATCATQRLANFLVHSSNNFGAILSSTNVGSNTY-$NH_2$; Daejeon, Republic of Korea). Ubiquitin was purchased from Sigma Aldrich (ubiquitin = MQIFVKTLTGKTITLEVEPSDTIENVKAKIQDKEGIPPDQQRLIFAGKQLEDGRTLSDYNIQKESTLHLVLRLRGG; St. Louis, MO, USA). Double distilled $H_2O$ ($ddH_2O$) was obtained from a Milli-Q Direct 16 system (Merck KGaA, Darmstadt, Germany). 1 sun light was treated from a Newport IQE-200 solar simulator (Irvine, CA, USA). ESI-MS and IM-MS analyses were performed using a Waters Synapt G2-Si quadrupole time-of-flight ion mobility mass spectrometer equipped with electrospray ionization source (DGIST Center for Core Research Facilities, Daegu, Republic of Korea) equipped with ESI source. NMR studies of Aβ with **Ir-1** were conducted on a Bruker Avance 600 MHz spectrometer equipped with a TCI triple-resonance inverse detection cryoprobe. The data was processed using TOPSPIN 2.1 (Bruker) and the assignment was performed using SPARKY 3.1134. Anaerobic reactions were performed in a $N_2$-filled glovebox (Korea Kiyon, Bucheon-si, Gyeonggi-do, Republic of Korea). Transmission electron microscopy (TEM) images were taken using a JEOL JEM-1400 transmission electron microscope (UNIST Central Research Facilities, Ulsan, Republic of Korea). Photophysical properties were measured by an Agilent Cary 100 UV-visible (UV-Vis) spectrophotometer and a Varian Cary Eclipse fluorescence spectrophotometer (UNIST Central Research Facilities, Ulsan, Republic of Korea). Time-correlated single photon counting (TCSPC) was performed for lifetime measurement with Ti:sapphire laser Mira900 (Coherent, Santa Clara, CA, USA), monochromator Acton series SP-2150i (Princeton Instruments, Acton, MA, USA), and TCSPC module PicoHarp 300 (PicoQuant, Berlin, Germany) together with MCP-PMT R3809U-59 (Hamamatsu, Shizuika-ken, Japan) and fitted by PicoQuant FluoFit software (UNIST Central Research Facilities, Ulsan, Republic of Korea).

### Synthesis of Ir-1

2-Phenylquinoline (680 mg, 3.3 mmol) was added to a solution of $IrCl_3{\cdot}nH_2O$ (500 mg, 1.7 mmol) in a mixture of 2-methoxyethanol and $H_2O$ (3:1). The solution was refluxed under $N_2$ (g) for 24 h. After cooling down to room temperature, brown precipitates were obtained. The crude product (the cyclometalated chloride-bridged $Ir^{III}$ dimer, $[Ir(C^\wedge N)_2(\mu\text{-}Cl)]_2$) was washed with hexanes and cold diethyl ether several times, dried, and used without further purification.[25]

A mixture of the cyclometalated chloride-bridged $Ir^{III}$ dimer (353 mg, 0.28 mmol), **1** (150 mg, 0.83 mmol), and $Na_2CO_3$ (294 mg, 2.8 mmol) was dissolved with 2-ethoxyethanol. The mixture was refluxed under $N_2$ (g) for 12 h. After cooling down to room temperature, the solution was concentrated followed by addition of water. The organic phase was extracted with $CH_2Cl_2$ three times. The collected organic solution was treated with $Na_2SO_4$ and removed under the reduced pressure. The crude materials were purified by column chromatography [$SiO_2$, 50:1 $CH_2Cl_2$:$CH_3OH$, $R_f$ = 0.6; red powder; 340 mg (yield 80%)]. $^1$H NMR [400 MHz, $CDCl_3$] $\delta$ (ppm): 8.79 (d, *J* = 8.0 Hz, 1H), 8.13 (t, *J* = 8.0 Hz, 1H), 8.07 (m, 3H), 7.92 (dd, *J* = 8.0 Hz, 1H), 7.80 (dd, *J* = 8.0 Hz, 1H), 7.70 (dd, *J* = 8.0 Hz, 1H), 7.67 (dd, *J* = 8.0 Hz, 1H), 7.51 (m, 2H), 7.42 (d, *J* = 8.0 Hz, 1H), 7.39 (ddd, 1H) 7.26 (ddd, 1H), 7.03 (m, 2H), 6.95 (m, 2H), 6.89 (dd, *J* = 8.0 Hz, 1H), 6.72 (m, 1H), 6.60 (dt, *J* = 6.8 Hz, 1H), 6.30 (m, 2H), 2.87 (s, 6H). $^{13}$C NMR [100 MHz, $CDCl_3$] $\delta$ (ppm): 173.0, 171.1, 169.2, 154.4, 151.8, 151.4, 148.7, 147.8, 147.0, 145.9, 145.1, 138.1, 136.3, 134.8, 129.4, 128.5, 126.0, 126.0, 125.2, 121.5, 120.5, 116.1, 109.7, 108.8, 39.1. FT-IR (neat $cm^{-1}$): 3057, 2021, 1608, 1516, 1437, 1381, 1338, 1163, 1028, 762. HRMS for $[M + Na]^+$ Calcd, 789.1812; found, 789.1814. UV/vis ($H_2O$): $\lambda_{max}$ ($\varepsilon$) = 463 nm (5.78 (± 0.12) x $10^3$ $M^{-1}cm^{-1}$). Elemental analysis calcd (%) for $C_{38}H_{29}IrN_4O_2{\cdot}0.5CH_3OH$: C 59.14, H 4.00, N 7.17; found: C 59.00, H 4.01, N 7.19.

### Electrospray Ionization Ion Mobility Mass Spectrometry (ESI-IM-MS)

$Aβ_{40}$, α-Syn, hIAPP, and ubiquitin (100 μM) were incubated with **Ir-1** or **1** (500 μM) in 100 mM ammonium acetate (pH 7.5) at 37 °C without any agitation. Incubated peptides were diluted by 10-fold and then injected into a mass spectrometer. The capillary voltage, sampling cone voltage, and source temperature were set to 2.8 kV, 70 V, and 40 °C, respectively. The backing pressure was adjusted to 3.2 mbar. Ion mobility wave height and velocity were adjusted to 10 V and 450 m/s, and gas flow for helium cell and ion mobility cell was set with 120 and 30 mL/min, respectively. Tandem MS ($MS^2$) analyses were additionally performed on the nonoxidized (Supporting Information, Figure S8) and singly/doubly oxidized peptides. The ESI parameters and experimental conditions were same as above. Collision-induced dissociation was conducted by

applying the collision energy in the trap and adjusting LM resolution to 15. More than 200 spectra were obtained for each sample and averaged for analyses. To estimate collision cross section values for obtained IM-MS data, calibration was also performed by following the previously reported procedures (Supporting Information, Figure S9).[26]

**Mass Spectrometric Analyses**

Oxidized $A\beta_{40}$, $\alpha$-Syn, hIAPP, and ubiquitin were observed upon incubation with **Ir-1** under aerobic conditions in the presence of light using a Waters Synapt G2-Si Q-Tof mass spectrometer equipped with electrospray ionization source. Only major charge states of all peptides (+3 for $A\beta_{40}$ and hIAPP, +9 for $\alpha$-Syn, and +5 for ubiquitin) are selected and shown in all mass spectra. Generally, exact mass should be calculated based on monoisotopic mass; however, in the present study, the oxidized peaks were assigned based on *m/z* values of the most abundant peaks because monoisotopic mass values of $\alpha$-Syn could not be well resolved without a high resolution mass spectrometer. For example, +3-charged $A\beta_{40}$ is most dominantly found in ESI-MS (Figure 2a). Upon treatment of **Ir-1** and light, the singly oxidized $A\beta_{40}$ ions were abundantly observed at 1449.6 *m/z* corresponding to a 16 Da increase in mass from the nonoxidized $A\beta_{40}$ peak at 1444.2 *m/z* (Figure 2a, bottom; blue). In the case of +9-charged $\alpha$-Syn at 1607.8 *m/z*, the singly oxidized peak is not well defined due to overlapping with sodiated ions at 1610.2 *m/z*. With the treatment of **Ir-1** and light, the doubly oxidized $\alpha$-Syn is found at 1611.3 *m/z* which indicates an approximate 32 Da increase in mass (Figure 2b, bottom; blue). The +3-charged hIAPP presents an oxidized peak at 1306.9 *m/z* indicating a 14 Da difference in mass from nonoxidized ions with 1302.2 *m/z* upon treatment with **Ir-1** and light (Figure 2c, bottom; blue). Different from $A\beta_{40}$ and $\alpha$-Syn, the singly oxidized hIAPP indicates a 14 Da increase in mass. In the ESI-MS spectra of ubiquitin, +5 charge state is the most abundantly detected (Figure S4 in Supporting Information). The singly and doubly oxidized ubiquitin is found at 1717.2 and 1720.3 *m/z*, respectively, which are approximately 16 and 32 Da increase in mass from nonoxidized ubiquitin centered at 1713.9 *m/z* (Supporting Information, Figure S4, bottom; blue).

## Acknowledgements

This work was supported by the 2016 UNIST research fund (1.160001.01) (to M.H.L., T.-H.K. & H.-W.R.); the National Research Foundation of Korea (NRF) Grant funded by the Korean Government [NRF-2014S1A2A2028270 (to M.H.L and A.R.); NRF-2014R1A2A2A01004877 and NRF-2016R1A5A1009405 (to M.H.L.)]; the Ministry of Science, ICT and Future Planning (KCRC 2014M1A8A1049320) (to J.C.). J.K. thanks the support from the Global Ph.D. fellowship program through the National Research Foundation of Korea (NRF) funded by the Ministry of Education (NRF-2015HIA2A1030823).

**Keywords:** Transition metal complexes • amyloidogenic peptides • photoactivation • peptide oxidation

[1] a) M. P. Lambert, A. K. Barlow, B. A. Chromy, C. Edwards, R. Freed, M. Liosatos, T. E. Morgan, I. Rozovsky, B. Trommer, K. L. Viola, P. Wals, C. Zhang, C. E. Finch, G. A. Krafft, W. L. Klein, *Proc. Natl. Acad. Sci. USA* **1998**, *95*, 6448-6453; b) M. G. Savelieff, A. S. DeToma, J. S. Derrick, M. H. Lim, *Acc. Chem. Res.* **2014**, *47*, 2475-2482; c) M. Baba, S. Nakajo, P.-H. Tu, T. Tomita, K. Nakaya, V. M.-Y. Lee, J. Q. Trojanowski, T. Iwatsubo, *Am. J. Pathol.* **1998**, *152*, 879-884; d) G. J. S. Cooper, B. Leighton, G. D. Dimitriadis, M. Parry-Billings, J. M. Kowalchuk, K. Howland, J. B. Rothbard, A. C. Willis, K. B. Reid, *Proc. Natl. Acad. Sci. USA* **1988**, *85*, 7763-7766; e) F. Chiti, C. M. Dobson, *Annu. Rev. Biochem.* **2006**, *75*, 333-366; f) D. M. Hartley, D. M. Walsh, C. P. Ye, T. Diehl, S. Vasquez, P. M. Vassilev, D. B. Teplow, D. J. Selkoe, *J. Neurosci.* **1999**, *19*, 8876-8884.

[2] a) S. I. A. Cohen, P. Arosio, J. Presto, F. R. Kurudenkandy, H. Biverstål, L. Dolfe, C. Dunning, X. Yang, B. Frohm, M. Vendruscolo, J. Johansson, C. M. Dobson, A. Fisahn, T. P. J. Knowles, S. Linse, *Nat. Struct. Mol. Biol.* **2015**, *22*, 207-213; b) S.-J. Hyung, A. S. DeToma, J. R. Brender, S. Lee, S. Vivekanandan, A. Kochi, J.-S. Choi, A. Ramamoorthy, B. T. Ruotolo, M. H. Lim, *Proc. Natl. Acad. Sci. USA* **2013**, *110*, 3743-3748; c) H. J. Lee, R. A. Kerr, K. J. Korshavn, J. Lee, J. Kang, A. Ramamoorthy, B. T. Ruotolo, M. H. Lim, *Inorg. Chem. Front.* **2016**, *3*, 381-392; d) J. S. Derrick, R. A. Kerr, Y. Nam, S. B. Oh, H. J. Lee, K. G. Earnest, N. Suh, K. L. Peck, M. Ozbil, K. J. Korshavn, A. Ramamoorthy, R. Prabhakar, E. J. Merino, J. Shearer, J.-Y. Lee, B. T. Ruotolo, M. H. Lim, *J. Am. Chem. Soc.* **2015**, *137*, 14785-14797; e) M. W. Beck, J. S. Derrick, R. A. Kerr, S. B. Oh, W. J. Cho, S. J. C. Lee, Y. Ji, J. Han, Z. A. Tehrani, N. Suh, S. Kim, S. D. Larsen, K. S. Kim, J.-Y. Lee, B. T. Ruotolo, M. H. Lim, *Nat. Commun.* **2016**, *7*, 13115. f) G. S. Yellol, J. G. Yellol, V. B. Kenche, X. M. Liu, K. J. Barnham, A. Donaire, C. Janiak, J. Ruiz, *Inorg. Chem.* **2015**, *54*, 470-475.

[3] a) A. Taniguchi, D. Sasaki, A. Shiohara, T. Iwatsubo, T. Tomita, Y. Sohma, M. Kanai, *Angew. Chem. Int. Ed.* **2014**, *53*, 1382-1385; b) M. Friedemann, E. Helk, A. Tiiman, K. Zovo, P. Palumaa, V. Tõugu, *Biochem. Biophys. Rep.* **2015**, *3*, 94-99; c) C. B. Glaser, G. Yamin, V. N. Uversky, A. L. Fink, *Biochim. Biophys. Acta* **2005**, *1703*, 157-169; d) W. Zhou, C. Long, S. H. Reaney, D. A. Di Monte, A. L. Fink, V. N. Uversky, *Biochim. Biophys. Acta* **2010**, *1802*, 322-330; e) V. N. Uversky, G. Yamin, P. O. Souillac, J. Goers, C. B. Glaser, A. L. Fink, *FEBS Lett.* **2002**, *517*, 239-244; f) M. Palmblad, A. Westlind-Danielsson, J. Bergquist, *J. Biol. Chem.* **2002**, *277*, 19506-19510; g) L. He, X. Wang, D. Zhu, C. Zhao, W. Du, *Metallomics* **2015**, *7*, 1562-1572; h) L. Hou, H. Shao, Y. Zhang, H. Li, N. K. Menon, E. B. Neuhaus, J. M. Brewer, I.-J. L. Byeon, D. G. Ray, M. P. Vitek, T. Iwashita, R. A. Makula, A. B. Przybyla, M. G. Zagorski, *J. Am. Chem. Soc.* **2004**, *126*, 1992-2005; i) L. Hou, I. Kang, R. E. Marchant, M. G. Zagorski, *J. Biol. Chem.* **2002**, *277*, 40173-40176; j) A. A. Watson, D. P. Fairlie, D. J. Craik, *Biochemistry* **1998**, *37*, 12700-12706; k) A. Taniguchi, Y. Shimizu, K. Oisaki, Y. Sohma, M. Kanai, *Nat. Chem.* **2016**, *8*, 974-982.

[4] a) S. R. Paik, H.-J. Shin, J.-H. Lee, *Arch. Biochem. Biophys.* **2000**, *378*, 269-277; b) S. Guedes, R. Vitorino, R. Domingues, F. Amado, P. Domingues, *Rapid Commun. Mass Spectrom.* **2009**, *23*, 2307-2315; c) D. G. Smith, R. Cappai, K. J. Barnham, *Biochim. Biophys. Acta* **2007**, *1768*, 1976-1990; d) K. Inoue, C. Garner, B. L. Ackermann, T. Oe, I. A. Blair, *Rapid Commun. Mass Spectrom.* **2006**, *20*, 911-918; e) M. Pietruszka, E. Jankowska, T. Kowalik-Jankowska, Z. Szewczuk, M. Smużyńska, *Inorg. Chem.* **2011**, *50*, 7489-7499.

[5] a) M. C. DeRosa, R. J. Crutchley, *Coord. Chem. Rev.* **2002**, *233–234*, 351-371; b) M. Tomita, M. Irie, T. Ukita, *Biochemistry* **1969**, *8*, 5149-5160; c) H.-R. Shen, J. D. Spikes, C. J. Smith, J. Kopeček, *J. Photochem. Photobiol. A* **2000**, *130*, 1-6; d) V. V. Agon, W. A. Bubb, A. Wright, C. L. Hawkins, M. J. Davies, *Free Radic. Biol. Med.* **2006**, *40*, 698-710; e) K. Huvaere, L. H. Skibsted, *J. Am. Chem. Soc.* **2009**, *131*, 8049-8060; f) J. E. Plowman, S. Deb-Choudhury, A. J. Grosvenor, J. M. Dyer, *Photochem. Photobiol. Sci.* **2013**, *12*, 1960-1967; g) C. Castaño, E. Oliveros, A. H. Thomas, C. Lorente, *J. Photochem. Photobiol. B* **2015**, *153*, 483-489; h) B. I. Lee, S. Lee, Y. S. Suh, J. S. Lee, A.-k. Kim, O.-Y. Kwon, K. Yu, C. B. Park, *Angew. Chem. Int. Ed.* **2015**, *54*, 11472-11476; i) S.-y. Takizawa, R. Aboshi, S. Murata, *Photochem. Photobiol. Sci.* **2011**, *10*, 895-903; j) K. Kim, D. A. Fancy, D. Carney, T. Kodadek, *J. Am. Chem. Soc.* **1999**, *121*, 11896-11897; k) D. A. Fancy, C. Denison, K. Kim, Y. Xie, T. Holdeman, F. Amini, T. Kodadek, *Chem. Biol.* **2000**, *7*, 697-708; l) F. Amini, C. Denison, H.-J. Lin, L. Kuo, T.

Kodadek, *Chem. Biol.* **2003**, *10*, 1115-1127; m) S. Meunier, E. Strable, M. G. Finn, *Chem. Biol.* **2004**, *11*, 319-326.

[6] a) E. Alarcon, A. M. Edwards, A. Aspee, C. D. Borsarelli, E. A. Lissi, *Photochem. Photobiol. Sci.* **2009**, *8*, 933-943; b) P. Drössler, W. Holzer, A. Penzkofer, P. Hegemann, *Chem. Phys.* **2003**, *286*, 409-420; c) E. Niu, K. P. Ghiggino, A. W.-H. Mau, W. H. F. Sasse, *J. Lumin.* **1988**, *40–41*, 563-564; d) J. A. Ferreira, R. Barral, J. D. Baptista, M. I. C. Ferreira, *J. Lumin.* **1991**, *48–49*, 385-390.

[7] J. S. Temenoff, H. Shin, P. S. Engel, A. G. Mikos, in *Proceedings of the Second Joint EMBS/BMES Conference*, **2002**, 687-688.

[8] a) M. Yoshimura, M. Ono, H. Watanabe, H. Kimura, H. Saji, *Sci. Rep.* **2014**, *4*, 6155; b) C.-W. Lee, M.-P. Kung, C. Hou, H. F. Kung, *Nucl. Med. Biol.* **2003**, *30*, 573-580; c) Z. Liu, P. J. Sadler, *Acc. Chem. Res.* **2014**, *47*, 1174-1185; d) Y. You, *Curr. Opin. Chem. Biol.* **2013**, *17*, 699-707; e) M. S. Lowry, S. Bernhard, *Chem. Eur. J.* **2006**, *12*, 7970-7977; f) H.-J. Zhong, L. Lu, K.-H. Leung, C. C. L. Wong, C. Peng, S.-C. Yan, D.-L. Ma, Z. Cai, H.-M. D. Wang, C.-H. Leung. *Chem*. *Sci*. **2015**, *6*, 5400-5408; g) T.-S. Kang, Z. Mao, C.-T. Ng, M. Wang, W. Wang, C. Wang, S. M.-Y. Lee, Y. Wang, C.-H. Leung, D.-L. Ma. *J*. *Med*. *Chem*. **2016**, *59*, 4026-4031; h) N. Onishi, S. Xu, Y. Manaka, Y. Suna, W.-H. Wang, J. T. Muckerman, E. Fujita, Y. Himeda. *Inorg*. *Chem*. **2015**, *54*, 5114-5123.

[9] I.-S. Shin, J. I. Kim, T.-H. Kwon, J.-I. Hong, J.-K. Lee, H. Kim, *J. Phys. Chem. C* **2007**, *111*, 2280-2286.

[10] K. L. Schey, E. L. Finley, *Acc. Chem. Res.* **2000**, *33*, 299-306.

[11] F. Lanucara, S. W. Holman, C. J. Gray, C. E. Eyers, *Nat. Chem.* **2014**, *6*, 281-294.

[12] S. Vijay-Kumar, C. E. Bugg, W. J. Cook, *J. Mol. Biol.* **1987**, *194*, 531-544.

[13] V. H. Wysocki, K. A. Resing, Q. Zhang and G. Cheng, *Methods* **2005**, *35*, 211-222.

[14] C. Schöneich, T. D. Williams, *Chem. Res. Toxicol.* **2002**, *15*, 717-722.

[15] A. M. Brown, J. A. Lemkul, N. Schaum, D. R. Bevan, *Arch. Biochem. Biophys.* **2014**, *545*, 44-52.

[16] N. Zhou, Z. Chen, D. Zhang, G. Li, *Sensors* **2008**, *8*, 5987-5995.

[17] A. Binolfi, A. Limatola, S. Verzini, J. Kosten, F.-X. Theillet, H. M. Rose, B. Bekei, M. Stuiver, M. van Rossum, P. Selenko, *Nat. Commum.* **2016**, *7*, 10251.

[18] C. W. Bertoncini, Y.-S. Jung, C. O. Fernandez, W. Hoyer, C. Griesinger, T. M. Jovin, M. Zweckstetter, *Proc. Natl. Acad. Sci. USA* **2005**, *102*, 1430-1435.

[19] S.-M. Liao, Q.-S. Du, J.-Z. Meng, Z.-W. Pang, R.-B. Huang, *Chem. Cent. J.* **2013**, *7*, 44-55.

[20] K. Garai, C. Frieden, *Proc. Natl. Acad. Sci. USA* **2013**, *110*, 3321-3326.

[21] a) P. Faller, C. Hureau, *Dalton Trans.* **2009**, *7*, 1080-1094; b) R. M. Rasia, C. W. Bertoncini, D. Marsh, W. Hoyer, D. Cherny, M. Zweckstetter, C. Griesinger, T. M. Jovin, C. O. Fernández, *Proc. Natl. Acad. Sci. USA* **2005**, *102*, 4294-4299; c) A. A. Valiente-Gabioud, V. Torres-Monserrat, L. Molina-Rubino, A. Binolfi, C. Griesinger, C. O. Fernández, *J. Inorg. Biochem.* **2012**, *117*, 334-341; d) J. R. Brender, K. Hartman, R. P. R. Nanga, N. Popovych, R. de la Salud Bea, S. Vivekanandan, E. N. G. Marsh, A. Ramamoorthy, *J. Am. Chem. Soc.* **2010**, *132*, 8973-8983. e) C. Cheignon, P. Faller, D. Testemale, C. Hureau, F. Collin, *Metallomics* **2016**, *8*, 1081-1089.

[22] Y.-P. Yu, P. Lei, J. Hu, W.-H. Wu, Y.-F. Zhao, Y.-M. Li, *Chem. Commun.* **2010**, *46*, 6909-6911.

[23] D. A. K. Traore, A. E. Ghazouani, L. Jacquamet, F. Borel, J.-L. Ferrer, D. Lascoux, J.-L. Ravanat, M. Jaquinod, G. Blondin, C. Caux-Thang, V. Duarte, J.-M. Latour, *Nat. Chem. Biol.* **2009**, *5*, 53-59.

[24] H. J. Bolink, E. Coronado, S. G. Santamaria, M. Sessolo, N. Evans, C. Klein, E. Baranoff, K. Kalyanasundaram, M. Graetzel, M. K. Nazeeruddin, *Chem. Commun.* **2007**, *31*, 3276-3278.

[25] M. Nonoyama, *Bull. Chem. Soc. Jpn.* **1974**, *47*, 767-768.

[26] B. T. Ruotolo, J. L. P. Benesch, A. M. Sandercock, S.-J. Hyung, C. V. Robinson, *Nat. Protoc.* **2008**, *3*, 1139-1152.

**Table of Contents**

FULL PAPER

**Turn-on oxidation power by light**: Oxidation of amyloidogenic peptides was achieved by an iridium(III) complex upon photoactivation under aerobic conditions, which was able to subsequently modulate their aggregation pathways.

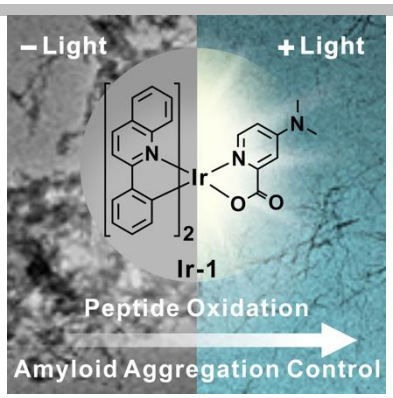


*Juhye Kang, Dr. Shin Jung C. Lee, Jung Seung Nam, Dr. Hyuck Jin Lee, Myeong-Gyun Kang, Kyle J. Korshavn, Hyun-Tak Kim, Jaeheung Cho, Prof. Dr. Ayyalusamy Ramamoorthy, Prof. Dr. Hyun-Woo Rhee,* Prof. Dr. Tae-Hyuk Kwon* and Prof. Dr. Mi Hee Lim**

***Page No. – Page No.***

**An Iridium(III) Complex as a Photoactivatable Tool for Oxidation of Amyloidogenic Peptides with Subsequent Modulation of Peptide Aggregation**